Journal of Hydroscience and Hydraulic Engineering
Vol. 9, No. 1, May, 1991, 11-26

SEASONAL THERMAL CYCLE IN STRATIFIED DEEP LAKES

By

K. Michioku

Kobe University, Rokkodai, Nada, Kobe, Japan

A. Murota

Osaka Industrial University, Daito, Osaka, Japan

and

S. Sakaguchi

Japanese Ministry of Construction

SYNOPSIS

Focusing on the thermo-dynamic processes in deep lakes, the annual cycle of thermal structure is analytically considered. An integral mixed-layer model is formulated to analyze the stratification and destratification processes. It is found that the annual thermal cycle in deep lakes is divided into the following three thermal stages: (1) the former heating period: temperature stratification develops due to water surface heating, (2) the latter heating period: the wind-induced mechanical stirring overcomes the stabilizing effect of surface heat flux and the mixed-layer slowly deepens under the action of weak vertical mixing and (3) the cooling period: the vertical mixing is driven by the combined action of the wind-generated disturbances and the thermal stirring caused by natural convection. The cooling period is, furthermore, divided into the two sub-categories: the mechanical-stirring-dominant period and the thermal-stirring-dominant period.

INTRODUCTION

Protection and improvement of hydraulic environment could be made by proper understanding of water mass and quality behavior. Although lakes and reservoirs play an important practical role in water resource engineering, little are understood about thermo-dynamic processes and mass transport mechanisms. Vertical mixing phenomena in a thermally stratified system are the most unknown factors among them. It is strongly desired to perform rational analyses for prediction of such processes, because their application to water quality prediction is of practical importance.

In order to obtain physical insight into the hydrodynamic mechanism in lakes, the authors carried out experimental studies concerning about two types of vertical mixing phenomena (1),(2). The first one is dealing with (i) vertical mixing in a thermally stratified system in which shear-free mechanical turbulence and stabilizing buoyancy flux were supplied from the top surface of a two-layer system. This situation corresponds to a stratified lake in heating period. The second experiment is dealing with (ii) vertical mixing induced by a combination of oscillating-grid stirring at the bottom and natural convection due to heating from below; this corresponds to a system in cooling season. The entrainment relationships for both of these situations were experimentally found. Numerical computation, using a turbulence closure model(3), were also performed to support these experimental results. These studies gave us information on turbulent heat transfer processes, which

could be much useful for performing analytical prediction of water quality behaviors in stratified lakes.

In this study, an analytical formulation of the mixing phenomena was performed for prediction of seasonally varying thermal structure in lakes. Focuses are placed on classification of thermo-dynamic phases of annual thermal cycle in lakes. Seasonal variation of meteorological factors imposed on lake surface assume to be composed of constant wind shear stress and annual variation of heat flux. The stratified temperature field is described by using a two-layer system composed of a uniformly mixed surface layer and a continuously stratified deep layer.

Normalizing the governing equations for the considering problem, we reduced several important dimensionless parameters which account for wind-induced mechanical stirring, surface heat exchange and thermal structure. Functional dependency of the mixing rate on these governing parameters was graphically presented for each thermal stage, which helps us to understand how external meteorological components, i.e. wind shear stress and surface heat flux, act on the thermal processes in lakes. It would appear that the present study help us to provide important informations for water quality problems concerning thermal stratification.

CONCEPT OF ANNUAL VARIATION OF THERMAL PROCESSES IN LAKES

Annual Thermal Cycle in Lakes

Fig. 1 is a schematic concept for the annual variation of energy gain and loss in a lake system, where the amount of energy supplied from atmosphere to lake is shown as a function of time. In Fig. 1, we define energy transfer from atmosphere to lake surface as positive energy. Energy is composed of two components, namely thermal (buoyant) and mechanical (or dynamic) energy fluxes. These two components of energies generate or suppress turbulent mixing, through which the turbulent kinetic energy is transformed into potential energy of density fields in lakes.

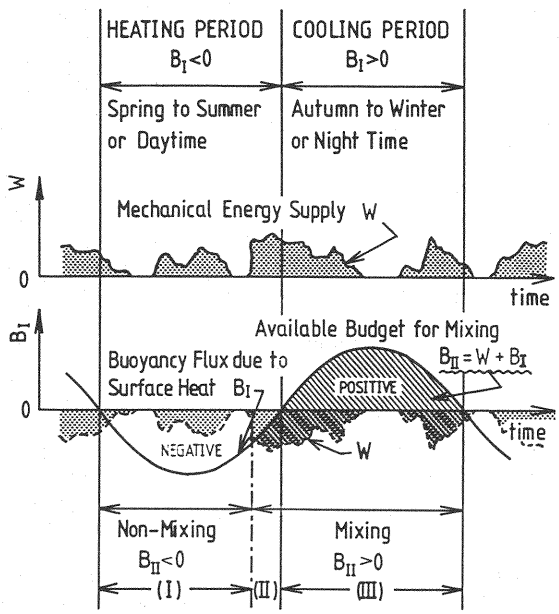

Fig.1 Concept of annual variation of energy gain and loss in a lake system

First, let us consider properties of mechanical energy. Time variation of the mechanical stirring due to wind stress W, is randomly as well as intermittently fluctuates, which always has a positive contribution to energy production.

Second, the buoyant energy flux due to surface heat exchange B_I (see the lower part of the figure) has two possibilities; in the cooling season, it supplies positive energy to generate the natural convection. On the other hand, during heating season, the buoyancy flux has a stabilizing effect to suppress the vertical mixing. The one year periodicity may be the most predominant time-dependent component in the buoyancy flux variation.

Then, available energy, being responsible for vertical mixing, might be $B_{I\,I}=W+B_I$. Through stratification and destratification processes, $B_{I\,I}$ is restored as potential energy of densimetric field in lakes.

These two external energy components act on a lake in quite different manners; the mechanical stirring plays a less important role on the entrainment process in a deeper mixed-layer, because mixing rate due to the mechanical turbulence energy monotonically decays with depth; on the other hand, the thermal convective motion is more active for a deeper mixed-layer. As a consequence, the thermal stirring is more predominant than the mechanical stirring when the thermocline is deep but it seldom affects the turbulent field when the mixed-layer is small.

Based on these considerations, the thermal process in lakes might be classified into the following three stages:

(I) The former heating season

In the beginning of the heating season, i.e. spring to early summer, the location of mixed-layer base is very deep, then the wind-generated turbulence is not so effective on interfacial mixing at the thermocline interface. The surface heat flux, however, increases the gravitational stability of the density field. In this situation, the negative contribution due to surface heat flux $B_I\ (\leq 0)$ overcomes the stirring effect of mechanical turbulence, W. Then, the total energy flux, $B_{I\,I}=W+B_I$, has negative contribution. A stably stratified thermal structure develops and little vertical mixing occurs in this stage.

(II) The latter term of heating season

With increasing the heating rate, the mixed-layer becomes thinner. After the peak heating rate, the magnitude of heating buoyancy flux, B_I, gradually decreases in turn. In this situation, the stirring effect of mechanical turbulence, W, becomes relatively important; it overcomes the stabilizing effect of heating buoyancy flux B_I. As a consequence, the total amount of energy, $B_{I\,I}=W+B_I$, becomes positive and thus it begins to generate turbulent motion and weak vertical mixing.

(III) Cooling season

In the cooling season, the buoyancy energy flux, B_I, also becomes positive, which produces natural convection. The vertical mixing is then induced by the combined action of the mechanical and thermal stirring (we will call it "composite stirring", from now on).

FORMULATION OF THEORETICAL MODEL

Vertical Mixing Rate

In our previous works(1),(2), the following two kinds of experiments were performed in order to obtain the entrainment relationships (see Fig.2):

(1) EXPERIMENT-I (Fig.2(a)(2))

The mechanical turbulence was generated by vertically oscillating a grid at the top surface of a two-layer system. At the same time, a stabilizing buoyancy flux was supplied by heating from above. The resulted mixing process

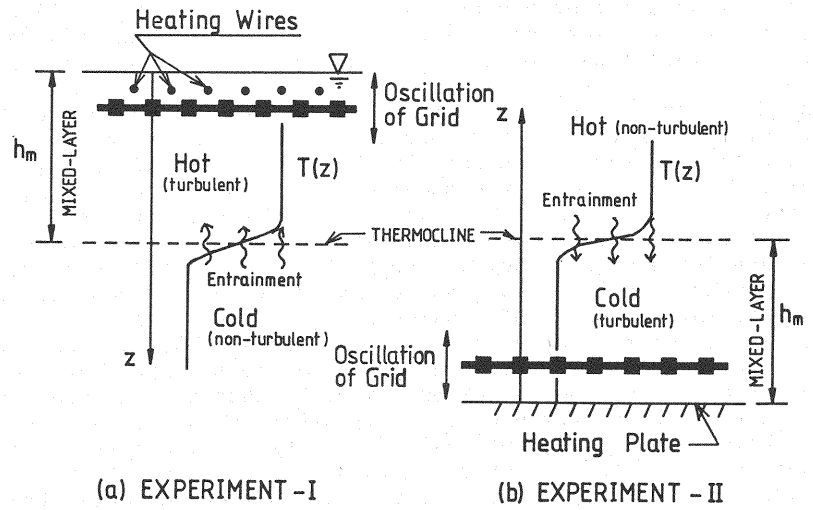

Fig.2 Schematic of the two experiments on entrainment processes in a two-layer thermal stratification system
(a) Experiment on vertical mixing with stabilizing buoyancy flux and shear free turbulence generated by a oscillating grid
(b) Experiment on vertical mixing with thermal convection and oscillating-grid turbulence

has a dynamic mechanism similar to that of the latter heating period (II). The following entrainment relationship was found:

$$E_{\sigma b} = C_1 R_{i\sigma b}^{-1}, \qquad (1)$$

where C_1 : empirically determined coefficient ($=1.10$), $E_{\sigma b}$: an entrainment coefficient ($=(dh_m/dt)/\sigma_b$), $R_{i\sigma b}$: an overall Richardson number ($=\varepsilon g l_s'/\sigma_b^2$), h_m : mixed-layer depth, t : time, ε : dimensionless density jump at the density interface, g : gravity acceleration, l_s' : integral length scale of the oscillating-grid turbulence at a density interface ($=\beta h_m$); its proportional coefficient, β, is found to be 0.1 (4) in this case. The velocity scale, measuring turbulence intensity, σ_b, in Eq.(1) is defined as follows.

$$\sigma_b = \left(u_s'^3 - \frac{u_b^3}{C_1 \eta_{b\theta}}\right)^{1/3} \qquad (2)$$

where, u_s' : intensity or r.m.s. velocity of oscillating-grid turbulence, $u_b=(-\alpha g F(t) h_m)^{1/3}$: a velocity scale of heating rate, $F(t)=F_h(t)/\rho c$ (℃ m/sec) : surface heat flux divided by product of density ρ and heat content of water c, $F_h(t)$: surface heat flux with a dimension of (cal/m^2), α : thermal expansion coefficient. The coefficient $\eta_{b\theta}$ was identified to be $\eta_{b\theta}=3.04$ through our experiment.

(2) EXPERIMENT-II (Fig.2(b))

The mixing process corresponding to the cooling season (III) was experimentally examined. ; The "composite stirring" was produced by using an oscillating grid and a heating plate both of which are installed at the bottom of the test tank. In this case, the entrainment relationship is given by

$$E_\sigma = C_2 R_{i\sigma}^{-1} \tag{3}$$

The entrainment coefficient and the overall Richardson number in this case are defined as $E_\sigma = (dh_m/dt)/\sigma$ and $R_{i\sigma} = \varepsilon g h_m/\sigma^2$. The scaling velocity σ is defined as

$$\sigma = (u_f^3 + \eta_\theta^3 u_s'^3)^{1/3} \tag{4}$$

where, $u_f = (\alpha g F(t) h_m)^{1/3}$ is a thermal convection velocity. A numerical value for η_θ is experimentally found to be *2.9*.

Although a closure assumption such as Eqs.(2) or (4) have also been used in several integral models for atmospheric, oceanic and lakes' mixed-layer, few of these models were experimentally verified. Our experimental and numerical works not only showed the validity of these assumptions but also proposed exact numerical values of unknown coefficients included in these formulas.

In order to apply these entrainment relationships to the practical system, the velocity scale of oscillating-grid turbulence should be converted to a friction velocity of wind shear stress, u_*. Using the analogy of Eqs.(2) and (4), the following entrainment relationships for the heating and cooling periods are respectively assumed:

$$\frac{dh_m}{dt} = C_w \frac{u_*^3}{\varepsilon g h_m} - C_b \frac{u_b^3}{\varepsilon g h_m} \tag{5}$$

$$\frac{dh_m}{dt} = C_w \frac{u_*^3}{\varepsilon g h_m} + C_f \frac{u_f^3}{\varepsilon g h_m} \tag{6}$$

These equations mean that the composite velocity scales defined by

$$\sigma_B = \{u_*^3 - (C_b/C_w) u_b^3\}^{1/3} \tag{7}$$

$$\sigma_F = (u_*^3 + (C_f/C_w) u_f^3)^{1/3} \tag{8}$$

play a dominant role for vertical mixing in the heating and cooling season, respectively.

The unknown coefficients, C_w, C_b and C_f, are determined as follows: First, the comparison between Eq.(5) and Eq.(1) leads to

$$C_w = C_1 \beta^{-1} (u_s'/u_*)^3 \tag{9}$$

$$C_b = (\eta_{b\theta}^3 \beta)^{-1} \tag{10}$$

From our experiment, $\eta_{b\theta} = 3.04$ and $\beta = 0.1$ were obtained. C_b is found to be $C_b = 0.356$. However, we have no reliable method to determine the numerical value of the relative turbulence intensity at the thermocline, u_s'/u_*. In this study, it is determined by using laboratory experimental results on wind-induced flow fields in closed two-layer density stratification systems (5),(6),(7),(8)). Their experimental data are shown in Fig.3. The following power law for the vertical distribution of $\sqrt{u'^2}$ is assumed,

$$\sqrt{u'^2}/u_* = C_u (z/h_m)^{-n} \tag{11}$$

and extrapolation of the best fit curve ($C_u = 1.0$ and $n = 0.3$) gives

$$\sqrt{u'^2}\,|_{z=h_m} = C_u u_* \tag{12}$$

Next, based on the assumption that "the entrainment relationship normalized in terms of turbulent scales is universal and it is independent on the mechanism of turbulence generation" (9), the turbulent intensity of the osci-

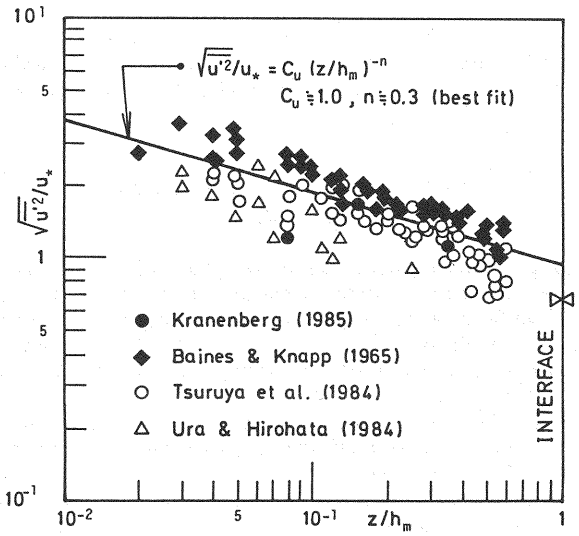

Fig.3 Vertical profiles of relative turbulence intensity, $\sqrt{u'^2}/u_*$ in closed two-layer density stratification systems. Details of experiments should be referred to 5),6),7),8).

llating-grid system u_s' is considered to be equivalent to that in the wind-shear flow system $\sqrt{u'^2}|_{z=h_m}$. Substituting Eq.(12) into u_s' in Eq.(9) we obtain $C_w = C_1 \beta^{-1} C_u^3 = 11.0$.

C_f can be identified by equating the thermal stirring components, i.e. the second term in Eq.(6), with that in Eq.(3). It is found to be $C_f = C_2 = 0.45$.

Summarizing the above discussion, the three coefficients included in Eqs.(5) and (6), are determined as

$$(C_w, C_b, C_f) = (11.0, 0.356, 0.45) \tag{13}$$

Another system which has similar mixing mechanism to that of a stratified lake system in cooling season is the convective boundary layer (CBL) in atmosphere. The vertical mixing in a CBL is driven by the combined action of heating from below and mechanical stirring due to friction at the ground surface. The capping inversion layer behaves as the thermocline in lakes. In some integral models for CBL, the same type of velocity scale is used:

$$\sigma' = \{u_f^3 + (C_F/C_A) u_*^3\}^{1/3} \tag{14}$$

Driedonks and Tennekes (10) proposed a numerical value of $C_F/C_A = 25.0$, which reasonably agrees well with our result, say, $C_w/C_f = 24.5$.

Heat Flux and Wind Shear (Fig.4)

External meteorological conditions are considerably simplified in order that we can easily parameterize external meteorological factors. A cyclic variation of surface heat flux $F(t)$ is approximated by a saw-tooth function similar to the analysis of Kraus and Turner (11) (see Fig.4). Although the wind shear stress, u_*, fluctuates randomly, it is assumed to be constant throughout the year.

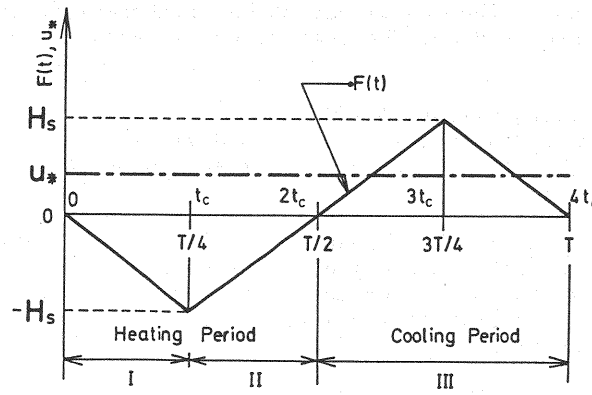

Fig.4 Assumed annual variation of heat flux and wind shear velocity in the present model.

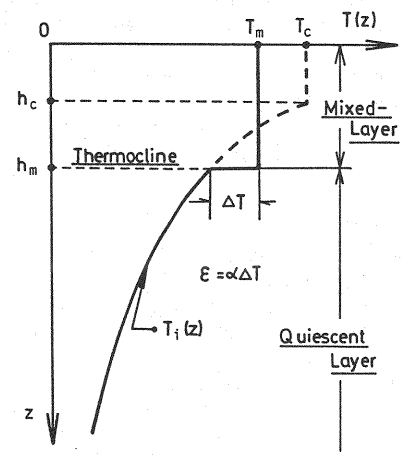

Fig.5 Temperature profile in the present analysis (broken line corresponds to the temperature distribution when the heating rate takes the peak value $F(t)=H_s$ at $t=t_c$.

Temperature Profile (Fig.5)

The temperature profile is described by an integral mixed-layer model, proposed by Kraus & Turner (11), which is shown in Fig.5. It is composed of a uniformly mixed surface layer and a continuously stratified deep layer. The two layers are bounded by a sharp thermocline with temperature jump ΔT. The entrainment rate across the thermocline is given by the entrainment laws Eqs.(5) and (6), where the specific density difference, ε, in these formulas is related to the temperature jump ΔT as

$$\varepsilon=\alpha\Delta T=\alpha\{T_m-T_i(h_m)\} \tag{15}$$

At the initial stage, it is assumed that the temperature field is homogeneous. We defined temperature, $T(z,t)$, to be a temperature deviation from the initial value.

As have discussed, the annual variation of thermal processes in lakes are divided into the three stages. The temperature in each stage is analyzed as follows.

(I) The former heating season ($0 \leq t \leq T/4$)

When we consider diurnal mixed-layer behaviors, the internal solar energy absorption in addition to surface heat flux should be taken into consideration, because the mixed-layer thickness might be less than or comparable to the depth scale of transparency. For the seasonal mixed-layer with several meters of thickness, however, internal heat flux at the mixed-layer base is negligibly small. In such a situation, solar energy input can be represented only by heat flux at the water surface. Then, the heat flux in the present analysis will be given only at the water surface.

The time-dependent heat flux, $F(t)$ is given by (see Fig.4)

$$F(t)=-H_s\, t/t_c \tag{16}$$

where, $t_c=T/4$: a quarter of a year and H_s : amplitude of heat flux.

In this case, only the surface water within a certain depth is stirred by the mechanical turbulence, because the stabilizing effect of heating buoyancy suppresses turbulent motion. Below this turbulent region, the system is not turbulent and a stable thermal stratification develops. Hence, it is considered that, at the bottom of the mixed-layer, the mechanical turbulence is completely balanced by the stabilizing buoyancy. In other words, the velocity scale which combines these two components, say σ_B in Eq.(7), becomes zero and thus no entrainment occurs at the bottom of the mixed-layer. The mixed-layer depth is then given by putting $\sigma_B=0$ as follows.

$$h_m=h_c\,(t/t_c)^{-1} \tag{17}$$

where, $h_c=C_w u_*^3/C_b \alpha g H_s$ is a depth scale characterizing the ratio of mechanical turbulence flux, u_*^3, to buoyancy energy flux, $\alpha g H_s$. For a larger depth scale h_c, the mechanical turbulence penetrates deeper. As seen in Eq.(17), h_m is inversely proportional to time and it takes the minimum value, h_c, at the time of peak heating flux, $t=t_c$.

On the other hand, the heat conservation in the mixed-layer gives

$$dT_m/dt=-F(t)/h_m \tag{18}$$

Substituting Eq.(16) into Eq.(18) and integrating it with the initial condition that $T_m=0$ at $t=0$, a solution for T_m is given by

$$T_m=(H_s\, t_c/3h_c)(t/t_c)^3 \tag{19}$$

The temperature profile in the deep layer, $T_i(z)$, is assumed to be unchanged. This is given by sets of $T_m(t)$ and $h_m(t)$ in the foregoing stage; the functional dependency of T_i on z is equivalent to the relationship between $T_m(t)$ and $h_m(t)$, where we let it be $T_i=T_m(t)$, $z=h_m(t)$ and t is treated as a dummy variable. Eliminating t in Eqs.(17) and (19) we get a solution of $T_i(z)$ as follows.

$$T_i(z)=H_s\, t_c\, h_c^2/3z^3 \qquad (\text{for } z \leq h_m) \tag{20}$$

One should note that, in this stage, there is no temperature jump, i.e. $\Delta T=0$.

As seen in the above analysis, the characteristic scales in the present system might be t_c, h_c and H_s. In terms of these variables, we define the following dimensionless parameters in order to generalize our discussion:

$$\tilde{t}=t/t_c,\ \tilde{z}=z/h_c,\ \tilde{h}_m=h_m/h_c,\ \tilde{T}_m=T_m h_c/H_s t_c, \tag{21}$$
$$\tilde{\varepsilon}=\varepsilon h_c/\alpha H_s t_c,\ \tilde{T}_i(z)=T_i(z) h_c/H_s t_c$$

Using these, the solutions Eqs.(17), (19) and (20) are rewritten in normalized forms as follows.

$$\tilde{h}_m = \tilde{t}^{1/2} \tag{22}$$

$$\tilde{T}_m = \tilde{t}^3/3 \tag{23}$$

$$\tilde{T}_i(z) = \tilde{z}^3/3 \tag{24}$$

(II) The latter heating season ($T/4 \leq t \leq T/2$)

The surface heat flux is given by (see Fig.4)

$$F(t_1) = -H_s(1 - t_1/t_c) \tag{25}$$

where, $t_1 = t - t_c$.

Strictly speaking, the stabilizing effect of heating flux could overcome the destabilizing effect of wind-shear stress even after the peak of heating rate. In other words, there could be régime, where the mixed-layer thickness increases under the conditions of $dh_m/dt = 0$ in Eq.(5) also during the latter heating season. In our later analysis (12), however, it is found that term of such a regime is quite short. That analysis showed us that the mixed-layer begins to deepen immediately after the peak heat flux. Based on such a information, it is assumed, in the present analysis, that the vertical mixing given by Eq.(5) begins just after $t = T/4$.

In this case, the rate of mixed-layer deepening is given by Eq.(5). Substituting the velocity scale $u_b = (-\alpha g F(t) h_m)^{1/3}$ and Eq.(25) into Eq.(5), we obtain

$$\frac{dh_m}{dt} = \frac{C_b \alpha g H_s \{h_c - (1 - \tilde{t}_1) h_m\}}{\varepsilon g h_m} \tag{26}$$

On the other hand, the heat conservation relationship from $t = t_c$ (or $t_1 = 0$) to $t = t_c + t_1$ (or $t_1 = t_1$) is given by

$$T_m h_m - \{T_c h_c + \int_{h_c}^{h_m} T_i(z)dz\} = -\int_0^{t_1} F(t)dt \tag{27}$$

where T_c is the mixed-layer temperature at $t = t_c$ (see Fig.5), which is given by Eq.(19) as $T_c = H_s t_c / 3h_c$. Substituting Eq.(25) into the right hand side of Eq.(27) and normalizing it by using Eq.(21), a solution for $\tilde{T}_m$ is obtained as:

$$\tilde{T}_m = (1/2 - 1/6\tilde{h}_m^2 + \tilde{t}_1 - \tilde{t}_1^2/2)/\tilde{h}_m \tag{28}$$

A solution for the specific density difference at thermocline $\tilde{\varepsilon}$ is obtained as

$$\tilde{\varepsilon} = \{(1 - \tilde{h}_m^{-2})/2 + \tilde{t}_1 - \tilde{t}_1^2/2\}/\tilde{h}_m \tag{29}$$

Substituting Eqs.(29) into Eq.(26) and normalizing it, a differential equation for $\tilde{h}_m$ is obtained as

$$\frac{d\tilde{h}_m}{d\tilde{t}_1} = C_b \frac{1 - (1 - \tilde{t}_1)\tilde{h}_m}{(1 - \tilde{h}_m^{-2})/2 + \tilde{t}_1 - \tilde{t}_1^2/2} \tag{30}$$

(III) Cooling season ($T/2 \leq t \leq T$)

The entrainment rate across the thermocline is given by Eq.(6). The same analytical procedures as the case of (II) can be applied to obtain a set of solutions. The results for the period of $(T/2 \leq t \leq 3T/4)$ are as follows.

$$\tilde{T}_m = (1 - 1/6\tilde{h}_m^2 - \tilde{t}_2^2/2)/\tilde{h}_m \tag{31}$$

$$\tilde{\varepsilon} = (1 - 1/\tilde{h}_m^2 - \tilde{t}_2^2/2)/\tilde{h}_m \tag{32}$$

$$\frac{d\tilde{h}_m}{d\tilde{t}_2} = \frac{C_b + C_f \tilde{h}_m \tilde{t}_2}{1 - 1/\tilde{h}_m^2 - \tilde{t}_2^2/2} \qquad (33)$$

where, $\tilde{t}_2 = t_2/t_c = \tilde{t} - 2$.

SOLUTION FOR ANNUAL VARIATION OF THERMAL STRUCTURE

Solutions for each thermal stage are obtained by numerically integrating those basic equations. The results are shown in Fig. 6. The abscissa shows the dimensionless time $\tau = \tilde{t}/4 = t/T$. The left-hand side of the vertical coordinates denotes the mixed-layer depth. The right-hand side represents the mixed-layer temperature, $\tilde{T}_m$, as well as the density jump at thermocline $\tilde{\varepsilon}$. All variables shown are normalized by Eq.(21). One can see that the mixed-layer becomes shallower and the thermal stratification develops during the heating period (Ⅰ); the mixed-layer depth takes the minimum value $\tilde{h}_m = 1$ at $\tau = 1/4$; just after that, the mixed-layer temperature takes the peak value ; the mixed-layer development is quite slow during the latter heating period (Ⅱ) and then it becomes rapid during the cooling phase (Ⅲ).

In order to verify the present analysis, the solution is compared with field data at Lake Chuzenji (13). The procedures are as follows.

The magnitude of heat flux, H_s, was evaluated by fitting the saw-tooth function curve to the observed heat flux, which is shown in the upper part of Fig.7. In this particular case, $H_s = 5.7\times10^{-5}$ (m℃/sec) is obtained. Although the friction velocity scale, u_*, should be determined from the time series of wind velocity through some statistical analyses, no useful method has been proposed to obtain a reasonable value for u_* so far. In this study, u_* is determined by using a regression method, so that the analytical solution in Fig.6 becomes the best fitting curves to the field data of thermal structure. The results are shown in the lower diagram of Fig.7. In this case, u_* is found to be $u_* = 4.0\times10^{-3}$ (m/sec). This corresponds to the situation that mean wind velocity at 10m above the water surface is approximately $u_{10} = 3.8$(m/sec), which seems to be a reasonable value for this lake. Despite such a rough evaluation in this analysis, the agreement between the predicted and observed thermal structure seems to be satisfactory.

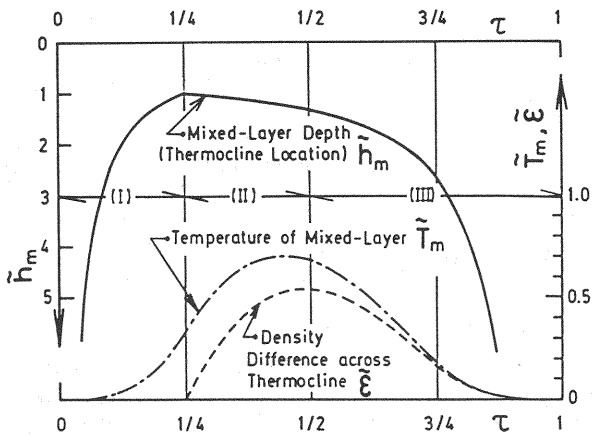

Fig.6 Solutions for mixed-layer depth $\tilde{h}_m$, its temperature, $\tilde{T}_m$ and specific density difference at the thermocline $\tilde{\varepsilon}$.

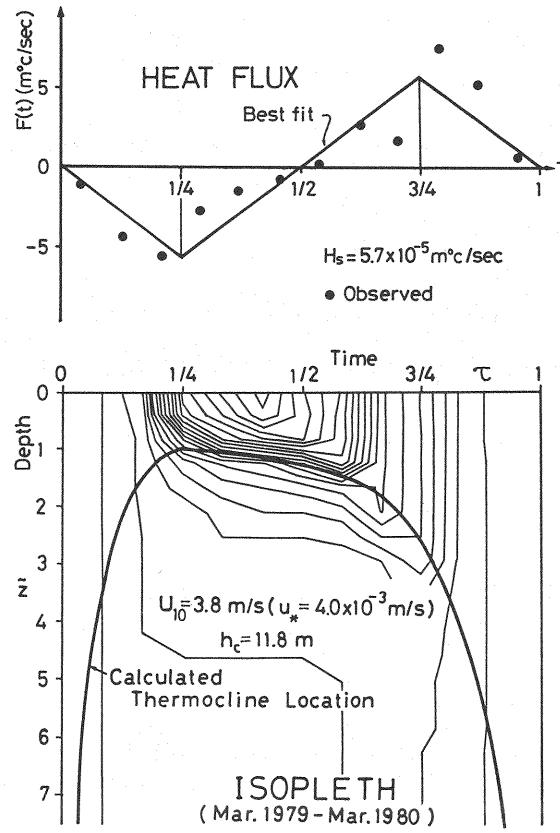

Fig.7 Comparison between the present analysis and the field data. (The upper diagram shows the field data of surface heat flux and its best fitting curve. The lower one represents the comparison between the observed isotherm (a set of thin lines) and the predicted thermocline location (a thick solid curve).

CLASSIFICATION OF THERMAL CYCLE IN LAKES

As seen in the above discussion, the behaviors of temperature fields in lakes are dependent on how much each of thermal and mechanical energy fluxes affect thermo-dynamic processes. In order to quantitatively show individual contribution to thermal structure development, we perform the following formulation on entrainment relationships.

First, we define new parameters of Froude-type which denote magnitude of external energy fluxes.

$$F_w = u_* / \sqrt{\varepsilon g h_m}\ , \qquad F_B = u_b / \sqrt{\varepsilon g h_m}\ , \qquad F_F = u_f / \sqrt{\varepsilon g h_m} \tag{34}$$

F_w, F_B and F_F shows the relative contribution of wind shear stress, heating thermal flux, and cooling thermal flux, respectively.

Second, the following two types of entrainment coefficients are defined:

Heating period

$$E_{\sigma B} = \frac{(dh_m/dt)}{\sigma_B} \quad , \quad \text{where } \sigma_B = (u_*^3 - \frac{C_b}{C_w} u_b^3)^{1/3} \tag{35}$$

Cooling period

$$E_{\sigma F} = \frac{(dh_m/dt)}{\sigma_F} \quad , \quad \text{where } \sigma_F = (u_*^3 + \frac{C_f}{C_w} u_f^3)^{1/3} \tag{36}$$

Eqs.(5) and (6), which are the entrainment rates for each thermal phase, can be rewritten in terms of these variables as follows.

Heating period : $E_{\sigma B} = C_w R_{i\sigma B}^{-1}$ (37)

Cooling period : $E_{\sigma F} = C_w R_{i\sigma F}^{-1}$ (38)

where, $R_{i\sigma B} = \varepsilon g h_m / \sigma_B^2$ and $R_{i\sigma F} = \varepsilon g h_m / \sigma_F^2$ are the corresponding overall Richardson numbers.

We can also rewrite these formulas by using the Froude numbers defined in Eq.(34) as.

Heating period : $E_{\sigma B} = C_w (F_w^3 - \frac{C_b}{C_w} F_B^3)^{2/3}$ (39)

Cooling period : $E_{\sigma F} = C_w (F_w^3 + \frac{C_f}{C_w} F_F^3)^{2/3}$ (40)

These equations give the functional dependency of entrainment coefficients, $E_{\sigma B}$ and $E_{\sigma F}$, on each external factors, say F_w, F_B and F_F. They are shown in Fig.8, where solid curves denotes contour lines for constant entrainment coefficients $E_{\sigma B}$ and $E_{\sigma F}$. Dotted curves are path lines of annual thermal cycles, which will be referred later.

Now, let us consider the thermal process during the former heating period (I). In this stage, mechanical energy production due to wind shear and energy loss due to stabilizing buoyancy flux are considered to have the same contribution to vertical mixing. No entrainment occurs in this case, say $dh_m/dt=0$ or $E_{\sigma B}=0$. Then, the functional relationship between F_B and F_w can be obtained by equating the entrainment rate in Eq.(39) to zero, which leads to

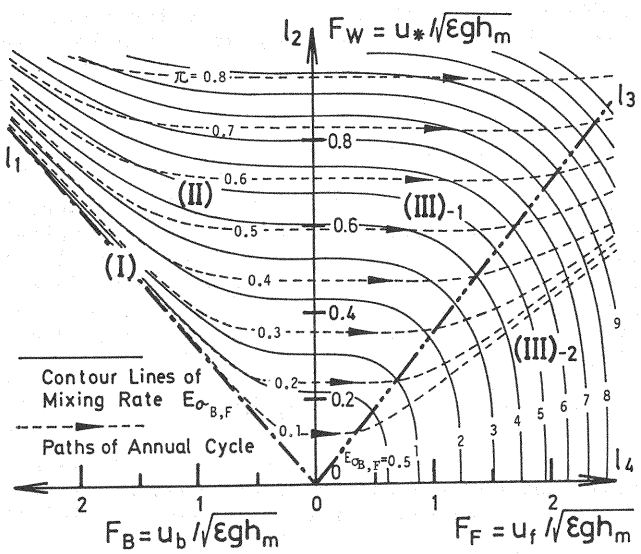

Fig.8 Iso-curves of entrainment coefficients, $E_{\sigma B}$ and $E_{\sigma F}$, (solid curves) and path lines of annual thermal cycle (dotted curves) in the (F_w, F_B, F_F)-plane.

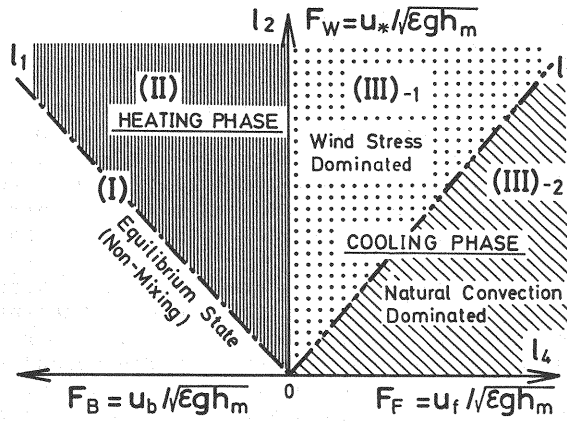

Fig.9 Schematic concept for regimes of annual thermal cycle.

$$F_v = (C_b / C_w)^{1/3} F_B \qquad (41)$$

Eq.(41) is shown in a thick chain line, l_1, in Fig.8. This is equivalent to an asymptotic curve that $E_{\sigma B} \to 0$. In the region between the line l_1 and F_B-axis, there is no mixing.

Second, let us consider the region bounded by l_1 and the vertical coordinate (l_2). This is corresponding to the latter heating period (II), where the mechanical energy is positive but the thermal buoyancy flux has negative contributions. In this case, a certain amount of mechanical energy is absorbed by stabilizing buoyancy flux and only the residual mechanical energy is available for vertical mixing.

Third, we consider another critical state that the wind-induced mechanical turbulence and the thermal convective motion has an equivalent stirring power. This situation is achieved when the first and the second terms in Eq.(14) (or in Eq.(40)) have the same magnitude. The functional relationship between F_v and F_F is given by equating the first term with the second term in Eq.(40). Then, we get

$$F_v = (C_f / C_w)^{1/3} F_F \qquad (42)$$

which is shown in a two-dotted chain line, l_3, in Fig.8. In the region above l_3, the mechanical stirring has more a predominant role on vertical mixing; on the other hand, in the region between l_3 and l_4 (F_F-axis), the thermal stirring is more effective in mixing.

A schematic of these categories in thermal processes is shown in Fig. 9, which can be summarized as follows.

(I) Former heating period (no mixing)
: on the line l_1,
(II) Latter heating period (weak mixing)
: between the lines l_1 and l_2,
(III)$_{-1}$ Former cooling period (mechanical stirring > thermal stirring)
: between the lines l_2 and l_3,
(III)$_{-2}$ Latter cooling period (mechanical stirring < thermal stirring)
: between the lines l_3 and l_4.

Now, we also show annual variation of the parameters, F_B, F_v and F_F, in the same plane as follows. By using the numerical solutions for mixed-layer development, say $\tilde{\varepsilon}(t)$ and $\tilde{h}_m(t)$, the time development of densimetric Froude numbers are written as follows,

$$F_w = \pi \tilde{\varepsilon}^{-1/2} \tilde{h}_m^{-1/2}$$
$$F_F = -F_B = (C_w/C_b)^{1/3} \{F(t)/H_s\}^{1/3} \pi \tilde{\varepsilon}^{-1/2} \tilde{h}_m^{-1/6} \quad (43)$$

where $\pi = u_* / \sqrt{\varepsilon_c g h_c} = u_* / \sqrt{\alpha g H_s t_c}$ is a new dimensionless parameter concerning the ratio of wind-induced stirring, u_*, to surface heat flux, H_s.

The functional relationships of $(F_w - F_B)$ and $(F_w - F_F)$ can be computed from Eq.(43), where time t is used as a dummy variable. These relationships for various values of π are represented dotted curves with arrows in Fig.8. These curves denote the path lines of annual thermal cycle in the $(F_w - F_B, F_F)$-plane.

One can see in this figure how the thermal cycle proceeds or how the thermal regime seasonally varies. During the former heating period, (I), values of $(F_B - F_w)$ change along the asymptotic line, l_1, (or zero-entrainment line), since there is no vertical entrainment. In the second stage, the latter heating period (II), the dotted curves begin to deviate upward from the line l_1, which indicates the entrainment rate $E_{c\,B}$ begins to increase. However, the path lines of annual variation (dotted curves) crosses the equi-value curves of the entrainment coefficient (solid curves) with rather a small angle, which shows that the increment of entrainment rate is still low in this stage. As the thermal regime is changing from the heating to the cooling season, and from the "wind-stress-dominant" stage to the "convection-dominant" stage, the cross angle between the path lines and the entrainment coefficients curves becomes larger, which means the vertical entrainment rate more rapidly increases.

CONCLUSION

The analytical model and the external meteorological conditions were considerably simplified under a constant wind-stress and a cyclic "saw-tooth" function of seasonal heat flux variation, so that we could generalize the discussion on annual thermal cycle in lakes. If one intends to obtain details of vertical temperature profiles in a certain lake, one should introduce some differential equation approaches rather than the integral model as well as employ the actual meteorological data as input conditions. The main purpose of the present study, however, is not to perform just a case study, which aims to find some regimes included in the thermal processes. By using primary characteristic scales for the annual thermal cycle and by performing an integral mixed-layer model analysis, several dimensionless governing parameters are found and thermo-dynamic processes in thermally stratified lakes are categorized into several stages.

In general, it is very difficult to obtain satisfactory meteorological and geometrical input data for water temperature prediction in lakes. In such a case, the present study could help us to make a rough estimation of seasonal variation of water temperature.

ACKNOWLEDGEMENT

The authors highly appreciate Prof. Dr. K. Muraoka, Osaka University, who allowed us to use the field data of Lake Chuzenji. This study was financially supported by Grant-in-Aid for Encouragement of Young Scientists (No.61750512).

The authors profoundly thank Mrs. Karen Schillinger, Karlsruhe, BRD, for helping us to prepare the manuscripts of this paper.

REFERENCES

1. Murota,A. and K.Michioku : Vertical mixing process in thermally stratified system induced by combined action of mechanical and thermal stirring, Proceedings of the 5th Congress of Asian and Pacific Regional Division of

International Association for Hydraulic Research, pp.183-202, 1986.
2. Murota,A. and K.Michioku : Dynamic effect of stabilizing buoyancy flux upon entrainment induced by oscillating-grid turbulence, Proceedings of the 6th Congress of Asian and Pacific Regional Division of International Association for Hydraulic Research, pp.177-184, 1988.
3. Murota,A. and K.Michioku : Numerical simulation of turbulent structure produced by combined action of mechanical and thermal stirring using a turbulence closure model, Refined Flow Modeling and Turbulence Measurement, Universal Academy Press, Inc., pp.395-402, 1989.
4. Thompson,S.M. and J.S.Turner : Mixing across an interface due to turbulence generated by an oscillating grid, Journal of Fluid Mechanics, Vol.67, pp.349-368, 1975.
5. Kranenburg,C. : Mixed-layer deepening in lakes after wind setup, Journal of Hydraulic Division, Proceedings of ASCE, HY 111, pp.1279-1297, 1985.
6. Baines,W.D. and D.J.Knapp : Wind driven water currents, Journal of Hydraulic Division, Proceedings of ASCE, HY91, pp.205-221, 1965.
7. Tsuruya,K. S.Nakano and H.Ichinohe : Interfacial mixing and turbulence characteristics in wind-induced currents, Proceedings of the 31st Congress of Coastal Engineering in Japan, pp.655-659, 1984 (in Japanese).
8. Ura,M. and K.Hirohata : Turbulent structure and entrainment phenomena in two-layered wind-induced currents, Proceedings of the 31st Congress of Coastal Engineering in Japan, pp.650-654, 1984 (in Japanese).
9. J.S.Turner : Buoyancy Effects in Fluids, Cambridge University Press, 1973.
10. Driedonks,A.G. and H.Tennekes : Entrainment Effects in the Well Mixed Atmospheric Boundary Layer, Boundary Layer Meteorology, Vol.30, pp.75-105, 1984.
11. Kraus,E.B. and J.S.Turner : A one-dimensional model of the seasonal thermocline, II .The general theory and its consequences, Tellus, 19, pp.98-105, 1967.
12. Michioku,K. and K.Kadoyu : Effect of Depth, Heat Flux and Mechanical Stirring upon Thermal Structure in Lakes, Proc. Hydraulic Engineering, Vol.34, 1990.
13. Muraoka,K. and T.Hirata : Thermal stratification and internal wave in Lake Chuzenji, Research Report from the National Institute for Environmental Studies, 69, pp.5-35, 1984.

APPENDIX - NOTATION

The following symbols are used in this paper.

$E_{\sigma B}$, $E_{\sigma F}$ = entrainment coefficients for heating and cooling periods, respectively;

$F(t)$ = heat flux (diveded by ρc) at the water surface;

F_v, F_B, F_F = dimensionless parameters of Froude-type which measure wind-shear, heating buoyancy flux and cooling buoyancy flux, respectively;

h_c = depth scale characterizing the ratio of mechanical turbulence flux to surface buoyancy flux.

h_m = mixed-layer depth;

H_s = magnitude of surface heat flux;

$R_{i\sigma B}$, $R_{i\sigma F}$ = overall Richardson numbers for heating and cooling periods, respectively;

t = time;

$T=4t_c=365(day)$ = one year time scale;

T_m = mixed-layer temperature;

$T_i(z)$ = temperature of deep layer;

u_b = velocity scale of surface heating;

u_f = velocity scale of natural convection;

u_* = friction velocity at the water surface;

z = vertical coordinate;

α = thermal expansion coefficient;

$\varepsilon = \alpha\Delta T$ = specific density difference across the thermocline;

σ, σ_B = turbulence velocity scale for heating and cooling periods, respectively;

$\pi = u_* / \sqrt{\alpha g H_s t_c}$ = dimensionless parameter denoting the ratio of wind-induced stirring to the surface heat flux;

and every "$\hat{\ }$"-capped symbol denotes dimensionless variables.

(Received August 27, 1990; revised January 30, 1991)